fluorescence-based assay (TaqMan) [14], pyrosequencing [15], single-base extension [16], matrix-assisted laser desorption/ionization time-of-flight mass spectrometry (MALDI-TOF MS) [17,18], and SNPlex assay [19]. However, many applications need to select relevant SNPs for their assay by in silico assay design, and some candidate SNPs are then excluded from investigation. Moreover, it is difficult or impossible for some assays to perform multiplex SNP genotyping.

To accomplish successful SNP typing for all candidate SNPs at low cost, new technologies must be developed. We previously reported a multiplex SNP typing method, designated the DigiTag assay, that has a high conversion rate (>90%) and reliable accuracy [20]. However, the DigiTag assay requires improvement with regard to simplifying assay protocols and reducing assay cost. In this study, we developed the DigiTag2 assay, which has simplified assay protocols, and performed typing for 96 SNP sites located in a 610-kb region on human chromosome 5 using 48 individual genomic DNA samples.

Materials and methods

DNA samples

Genomic DNA samples from 48 unrelated healthy donors were obtained from the Japan Health Science Foundation (Osaka, Japan). All donors provided written informed consent, and samples were anonymized. For each sample, 1 μg of purified genomic DNA was dissolved in 20 μl of TE buffer (pH 8.0, Wako, Osaka, Japan) for use and was stored at −20 °C.

End digits and first digits

We designed the end digits (EDs) and first digits (D1s) to be 23-mer oligonucleotides and attached the EDs and D1s to 5′ query probes and 3′ query probes, respectively. We prepared two EDs (ED-1 and ED-2) for two alleles at each SNP. All EDs and D1s are used for the priming site in the labeling step, and D1s are also used as probes that are attached to DNA microarray in the detection step. The EDs and D1s have the following properties: (i) uniform melting temperature (58.8 ± 1.0 °C) and length, (ii) specific hybridization only to complementary EDs and D1s, (iii) minimal interaction with other EDs and D1s, and (iv) no formation of secondary structures [21]. These properties ensure uniform polymerase chain reaction (PCR) efficiency, even if all of the EDs and D1s are used in multiplex PCR. Furthermore, precise hybridization on DNA microarray is possible using a set of D1s with high reproducibility. Sequence information for EDs and D1s is listed in Supplementary Table 1.

Multiplex PCR from sample DNA

We designed multiplex PCR primers for each of the 96 SNP sites to have relatively long length (average length 40-mer) and to give PCR products of between 181 and 798 bp (average length 527 bp). Sequence information for the multiplex PCR primers is listed in Supplementary Table 2.

We performed multiplex PCR using a two-step protocol (denature and extension steps) with a 6-min extension step using specifically designed primer pairs. Multiplex PCR was performed with 2.5 μl genomic DNA and 250 fmol of each primer for 96 SNP sites in 10 μl of 2× Qiagen Multiplex PCR Master Mix containing HotStarTaq DNA polymerase, multiplex PCR buffer and deoxynucleoside triphosphate (dNTP) mix (Qiagen Multiplex PCR Kit, Qiagen, Valencia, CA, USA). Cycling was performed using a Bio-Rad PTC-200 Peltier thermal cycler (Bio-Rad, Hercules, CA, USA) as follows: 95 °C for 15 min, followed by 40 cycles of 95 °C for 30 s and 68 °C for 6 min. When necessary, fragment length of the 96 PCR products was confirmed by capillary electrophoresis (Agilent 2100 Bioanalyzer, Agilent, Palo Alto, CA, USA) to evaluate PCR efficiency.

Encoding reaction

We performed multiplex oligonucleotide ligation assay using the multiplex PCR products as targets. For 96-plex oligonucleotide ligation assay, we prepared mismatch-induced 5′ query probes for 91 target SNPs and perfect match 5′ query probes for 5 target SNPs (SNP 7, SNP 9, SNP 18, SNP 49, and SNP 93). The assignment of D1s to the SNPs analyzed in this study and sequence information for the probes are listed in Supplementary Table 3.

Prior to the encoding reaction, 96 unmodified 3′ query probes were simultaneously phosphorylated at the 5′ end in 40 μl of 1× protruding end kinase buffer containing 30 mM adenosine triphosphate (ATP), 40 U polynucleotide kinase, and 4 pmol of 3′ query probes for 96 SNP sites (Kination Kit, Toyobo, Osaka, Japan). The reaction mixture was incubated for 30 min at 37 °C and for 3 min at 95 °C using a Bio-Rad PTC-200 Peltier thermal cycler. The encoding reaction was prepared by mixing 1 μl of multiplex PCR products in 15 μl of *Taq* DNA ligase buffer containing 20 mM Tris–HCl (pH 7.6), 25 mM potassium acetate, 10 mM magnesium acetate, 10 mM dithiothreitol (DTT), 1 mM nicotinomide adenosine dinucleotide (NAD), and 0.1% Triton X-100 (New England Biolabs, Beverly, MA, USA) with 10 fmol of probes (192 5′ query probes and 96 phosphorylated 3′ query probes) and 10 U *Taq* DNA ligase. All components of the encoding reaction were mixed on ice. The encoding reaction initially was held at 95 °C for 5 min, followed by 58 °C for 15 min using a Bio-Rad PTC-200 Peltier thermal cycler. The reaction was stopped by holding the temperature at 10 °C.

Labeling reaction

For the labeling reaction, 6 μl of ligation products was directly mixed in 12 μl of *Ex Taq* buffer containing 20 mM Tris–HCl (pH 8.0), 100 mM KCl, 0.1 mM ethylenediaminetetraacetic acid (EDTA), 1 mM DTT, 0.5% Tween 20, 0.5%

Nonidet P-40, 50% glycerol, and 2 mM each dNTP (TaKaRa, Shiga, Japan) with 6.0 pmol of Cy3-labeled ED-1 (Cy3–ED-1), 6.0 pmol of Cy5-labeled ED-2 (Cy5–ED-2), 30 fmol each of the 96 D1s, and 1.5 U *Ex Taq* polymerase. The reaction initially was incubated at 95 °C for 1 min, followed by 30 cycles of 95 °C for 30 s, 55 °C for 6 min, and 72 °C for 30 s, using a Bio-Rad PTC-200 Peltier thermal cycler. The reaction was stopped by holding the temperature at 10 °C.

Hybridization and detection on DNA microarray

We purchased a DNA microarray (NovusGene, Tokyo, Japan) that had 24 separated areas on the same slide glass. Each of the separated areas contained 100 types of oligonucleotide probe (96 probes for 96 SNPs and 4 probes for validation controls of the assay) identical to D1 sequences. Of the 4 validation control probes, 3 were not used in the DigiTag2 assay because these probes were prepared to validate the washing step with magnetic beads in the previous version of the DigiTag assay. The ready-to-use DNA microarrays were stored in a desiccator at room temperature until use.

A hybridization mixture was prepared by mixing 5 μl of labeled products in 12 μl of hybridization buffer containing 0.5× SSC, 0.1% sodium dodecyl sulfate (SDS), 15% formamide, and 1 mM EDTA with 1 μl of hybridization control. The hybridization control was prepared with 2.5 fmol of Cy3-labeled D1_100 and Cy5-labeled D1_100. Then 8 μl of the hybridization mixture was applied to each area on the DNA microarray. Hybridization was carried out for 30 min at 37 °C in a hybridization oven (ThermoStat plus, Eppendorf, Hamburg, Germany). After hybridization, DNA microarrays were washed in washing buffer (0.1× SSC and 0.1% SDS) with shaking at 60 rpm for 5 min. DNA microarrays were consecutively washed in distilled water with shaking at 60 rpm for 1 min and were then dried by centrifugation at 2000 rpm for 1 min. Hybridization images were scanned at photomultiplier voltages of 400 V for Cy3 and 480 V for Cy5 using a commercially available DNA chip scanner, and fluorescence image analysis was performed using commercially available software (GenePix 4000B unit and GenePix Pro 4.1 software package, Axon Instruments, Foster City, CA, USA). The genotype calls were determined using the SNPStar software (version 0.0.0.8, Olympus, Tokyo, Japan).

Results and discussion

DigiTag2 assay scheme

We previously reported a multiplex SNP typing method, the DigiTag assay, in which all of the SNP genotypes are encoded to the well-designed oligonucleotides, named DNA coded numbers (DCNs) [20]. The assignment of the DCNs to the SNPs is unconstrained; therefore, the DNA chips prepared to read out the types of DCN are universally available for any types of SNP. We revealed that the DigiTag assay has the potential to analyze nearly all kinds of SNP with high accuracy and reproducibility. However, the DigiTag assay needs the washing step with magnetic beads, which is a laborious step in manipulation. Also, the biotinylated probes, which are necessary for the washing step, are expensive. For the next version of the assay, we improved the protocol to exclude the washing step and named it the DigiTag2 assay.

The DigiTag2 assay involves four steps to accomplish the genotyping: target preparation, encoding, labeling, and detection (Fig. 1). During target preparation, target fragments (including target SNP sites) are prepared by multiplex PCR from genomic DNA. For multiplex PCR, we designed 40-mer primers (average length) and performed multiplex PCR using a two-step protocol (denature and extension steps) with a 6-min extension step. For encoding, we prepared two 5′ query probes and one 3′ query probe for each SNP site. The 5′ query probes have a sequence

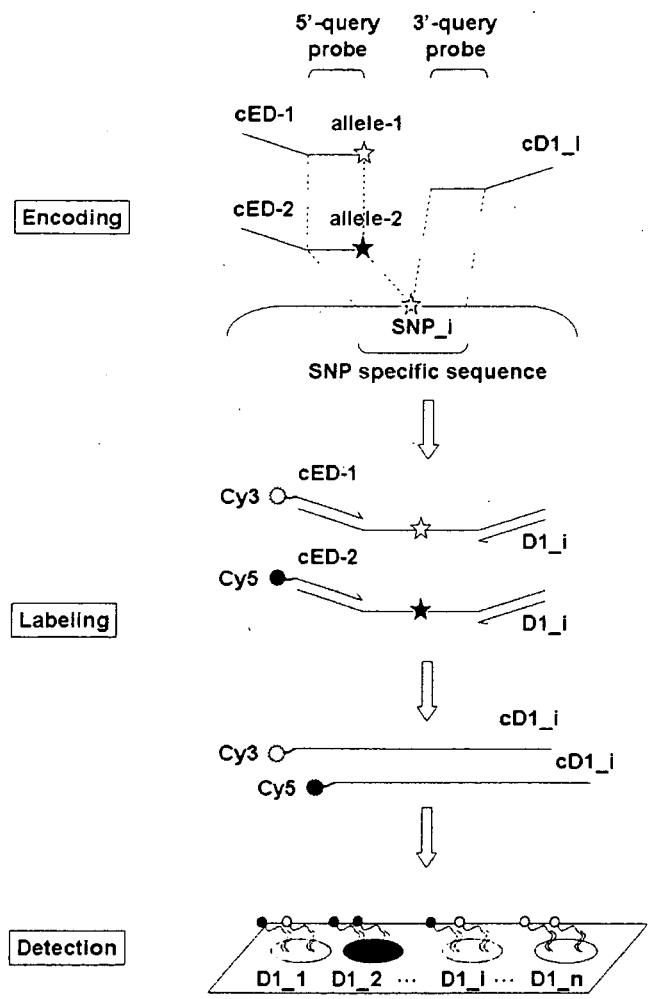

Fig. 1. Schematic representation of DigiTag2 assay. This assay involves four steps to accomplish SNP typing: target preparation, encoding, labeling, and detection. The 5′ query probes have EDs (cED-1 and cED-2) corresponding to each allele, and the 3′ query probes have a variable sequence (cD1_i) for each SNP. Each reverse complement sequence is depicted by a lowercase "c" before the sequence name.

complementary to the 5′-flanking region of the target SNP, and each of the probes has an allele-specific sequence. Two types of ED (ED-1 and ED-2) were attached to each of the 5′ query probes (see Materials and Methods), and we incorporated a mismatch base into the 5′ query probes at the fourth position from the SNP site to improve the precision of allele discrimination [20]. The 3′ query probe has a sequence complementary to the 3′-flanking region of the target SNP, and each of the probes has a D1 on its 3′ end. In the encoding step, the 5′ query and 3′ query probes are successfully concatenated by *Taq* DNA ligase, and the probes are fully complementary to adjacent regions on the target fragment [22]. The genotype is then converted into a type of ED and a type of D1. The types of ED and D1 designate the type of allele and SNP, respectively. After the encoding step, fluorescence is incorporated into the ligated products by asymmetric PCR using fluorescent-labeled primers (Cy3-ED-1 and Cy5-ED-2) and D1 primers. The D1 primers are a mixture of all D1s used in the assay. The Cy3- and Cy5-labeled PCR products are directly hybridized with the D1 probes on the DNA microarray to reveal SNP genotypes by reading signals from the various D1s. If the genomic DNA sample is homozygous for a certain SNP, a single color signal from Cy3 or Cy5 is detected from the corresponding spot on the DNA microarray. In contrast, both signals are present when the genomic DNA sample is heterozygous.

SNP selection and probe design

In a previous report, we investigated the ligation conditions in the encoding step using an SNP located in the *PLOD* gene on human chromosome 1p36 as a model SNP (JSNP ID IMS-JST068774) and determined the parameters for 5′ query and 3′ query probes [20]. We then randomly selected 96 SNPs from a 610-kb region, including the *IL-4* and *IL-13* genes on human chromosome 5q31-33, which contains various candidate genes related to immune and allergic disorders. We subsequently designed probes for the 96 SNP sites to have a uniform melting temperature as that of *PLOD* SNP so as to give similar ligation efficiency among the 96 SNP sites to be analyzed in a single tube. We also incorporated a mismatch base into the 5′ query probe at the fourth position from the SNP site for all target SNPs. The 20-mer mismatch-induced 5′ query probes and 3′ query probes (average length) had melting temperatures of 50.7 ± 2.1 °C and 52.4 ± 1.5 °C, respectively. Here we found that the length of the 3′ query probe influences the ligation efficiency in the encoding step; when a longer 3′ query probe was used in the encoding step, stronger signal intensities were acquired on microarray detection (data not shown). Therefore, we used the lengthened 3′ query probes to 30-mer, and the average melting temperature of the lengthened 3′ query probes was 66.1 ± 3.5 °C. The sequence information for 5′ query probes and lengthened 3′ query probes is listed in Supplementary Table 3.

Optimization of reaction conditions

When we used the mismatch-induced 5′ query probes, indistinct clusters were observed from 5 SNPs (SNP 7, SNP 9, SNP 18, SNP 49, and SNP 93) (Fig. 2A). However, these 5 SNPs can be discriminatively genotyped with perfect

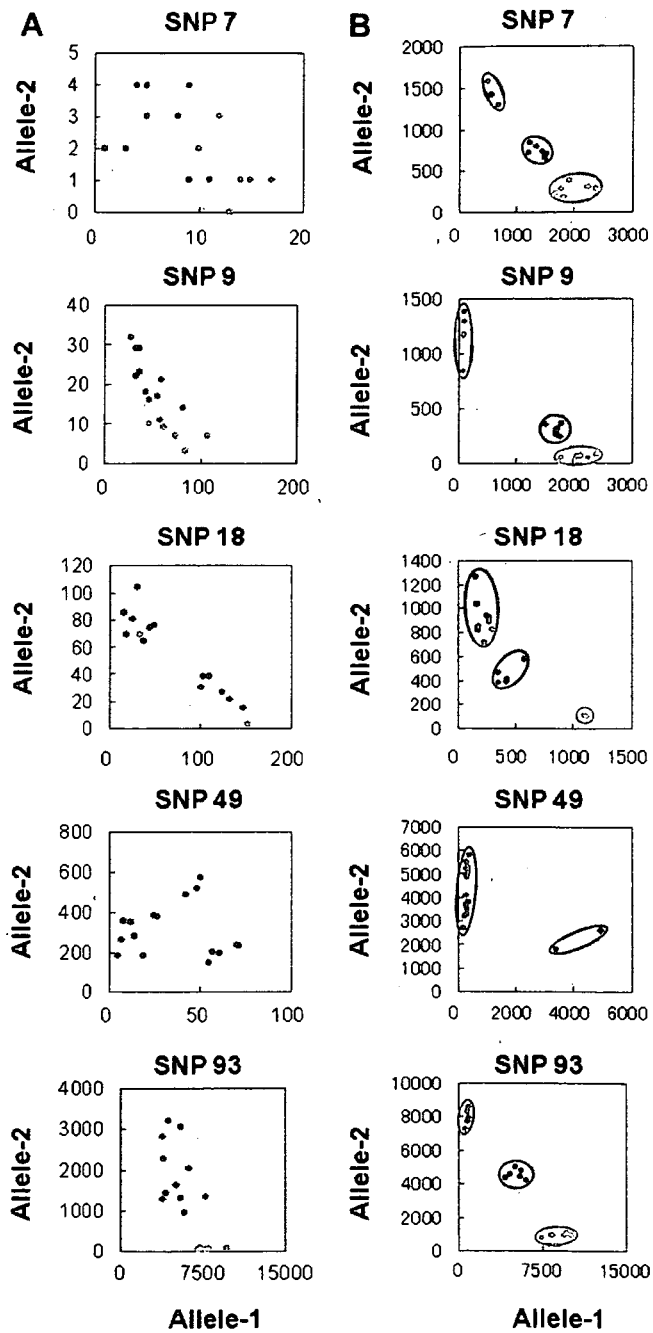

Fig. 2. Treatment of 5 failed SNPs with mismatch-induced 5′ query probes. Green dots and circle show allele-1 homozygous samples, red dots and circle show allele-2 homozygous samples, and blue dots and circle show heterozygous samples. (A) Mismatch-induced 5′ query probes, which have a mismatched base incorporated into the fourth position from the SNP base, were used. (B) Here 5′ query probes, which have a perfect match sequence for the target SNP, were used instead of mismatch-induced 5′ query probes.

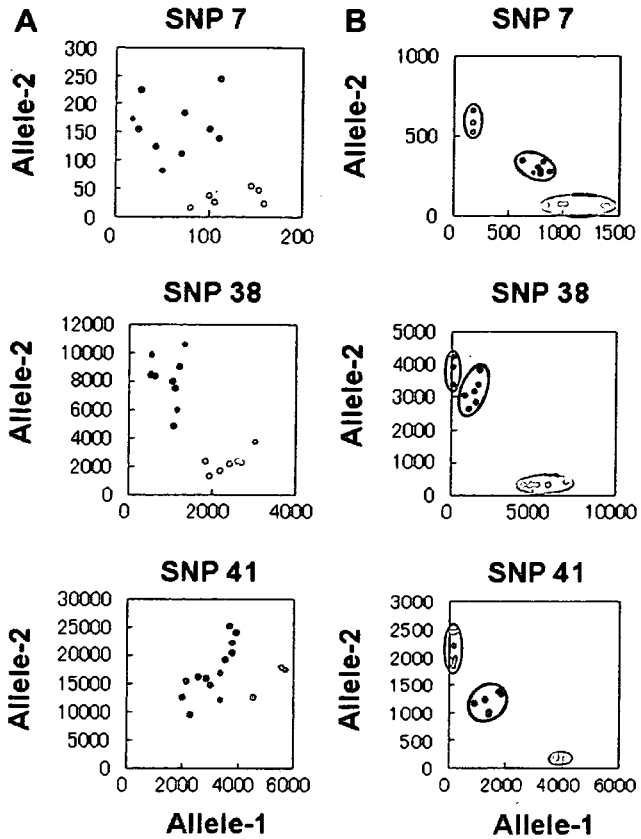

Fig. 3. Effects of D1 primer concentration in the labeling step. Green dots and circle show allele-1 homozygous samples, red dots and circle show allele-2 homozygous samples, and blue dots and circle show heterozygous samples. (A) Here 5 nM D1 primers was used with 500 nM fluorescent-labeled primers. (B) Here 2.5 nM D1 primers was used with 500 nM fluorescent-labeled primers.

match 5′ query probes (Fig. 2B). For these 5 SNPs, the mismatch base incorporated into the fourth position from the SNP site has a drastic effect on the hybridization stability between 5′ query probes and the target multiplex PCR products in the encoding step and leads to signal loss on microarray detection. Therefore, we performed a 96-plex oligonucleotide ligation assay with the mismatch-induced 5′ query probes for 91 target SNPs in combination with perfect match 5′ query probes for these 5 target SNPs.

To incorporate the fluorescent label into the ligated products, we performed asymmetric PCR with fluorescent-labeled primers and D1 primers (mixture of D1s). Using the mixture of all D1s, instead of the single primer pair mentioned in the DigiTag assay [20], would make it possible to uniformly acquire all target fragments. However, the concentration of D1 primers used in the labeling step was found to exert an influence on the cluster distribution in scatter diagrams. When we used 5 nM D1 primers with 500 nM fluorescent-labeled primers, dispersed and/or indiscrete clusters were observed for several SNPs (Fig. 3A). However, the dispersed and/or indiscrete clusters became convergent and/or discrete clusters when we used 2.5 nM D1 primers with 500 nM fluorescent-labeled primers (Fig. 3B). The D1 primers share the fluorescent-labeled primers in the labeling step, and the ratio of each D1 primer to fluorescent-labeled primer was approximately 1:2 at 2.5 nM and 1:1 at 5 nM. When the amount of each D1 primer was greater than the amount of fluorescent-labeled primer, strong false-positive signals were observed on microarray detection, leading to indiscrete clusters on scatter diagrams (data not shown). On the other hand, when the amount of each D1 primer was less than the amount of fluorescent-labeled primer, insufficient amplification occurred in a number of target SNPs, leading to weak signal intensities on microarray detection (data not shown). We found that the optimal ratio of D1 primer to fluorescent-labeled primer is approximately 1:2, irrespective of the multiplicity of the assay (number of SNPs to be analyzed).

Genotyping results

Multiplex PCR products, including the 96 SNP sites, showed similar band patterns as 48 individual DNA samples, although it was difficult to clearly discern all 96 PCR products due to limitations in electrophoretic resolution (Fig. 4A). We then performed a multiplexed oligonucleotide ligation assay using the multiplex PCR products as targets. To incorporate the fluorescent label into the ligated products, asymmetric PCR was performed using the fluorescent-labeled and D1 primers. DNA microarray revealed hybridization images of 24 individual samples from each of the 24 separated areas having 100 spots (96 probes for 96 SNPs and 4 probes for validation controls) (Fig. 4B). The hybridization image was analyzed using a DNA chip scanner, and the Cy3 and Cy5 signal intensities of each spot were plotted to produce a scatter diagram. The SNP genotypes of 16 genomic DNA samples, randomly selected from the 48 samples, were alternatively determined by direct sequencing and were used as reference data.

As a result of 96-plex genotyping under optimal labeling conditions using the mismatch-induced 5′ query probes in combination with the perfect match 5′ query probes for 5 SNPs, three distinct clusters corresponding to two homozygous genotypes and one heterozygous genotype were observed from 84 SNPs (exceptions were SNP 31, SNP 37, SNP 60, SNP 61, and SNP 87) (Fig. 4C). The remaining 7 SNPs (SNP 12, SNP 22, SNP 27, SNP 33, SNP 67, SNP 88, and SNP 91) were found to be monomorphic in 48 genomic DNA samples and were excluded from further analysis. For SNP 37, SNP 60, and SNP 87, drastically attenuated signal intensities were observed on microarray detection (Fig. 4D). Signal loss was caused by insufficient amplification of the target fragments on multiplex PCR because no amplified products were observed on singleplex PCR, even when the second candidate primer pairs were used. There were some structural obstacles in the target region, although we could not identify any characteristic structures. SNP 31 and SNP 61 were found to have strong false-positive signals, leading to indistinct clusters on scatter diagrams (Fig. 4E). The false-positive signals would be caused by the misligation in the encoding step that was

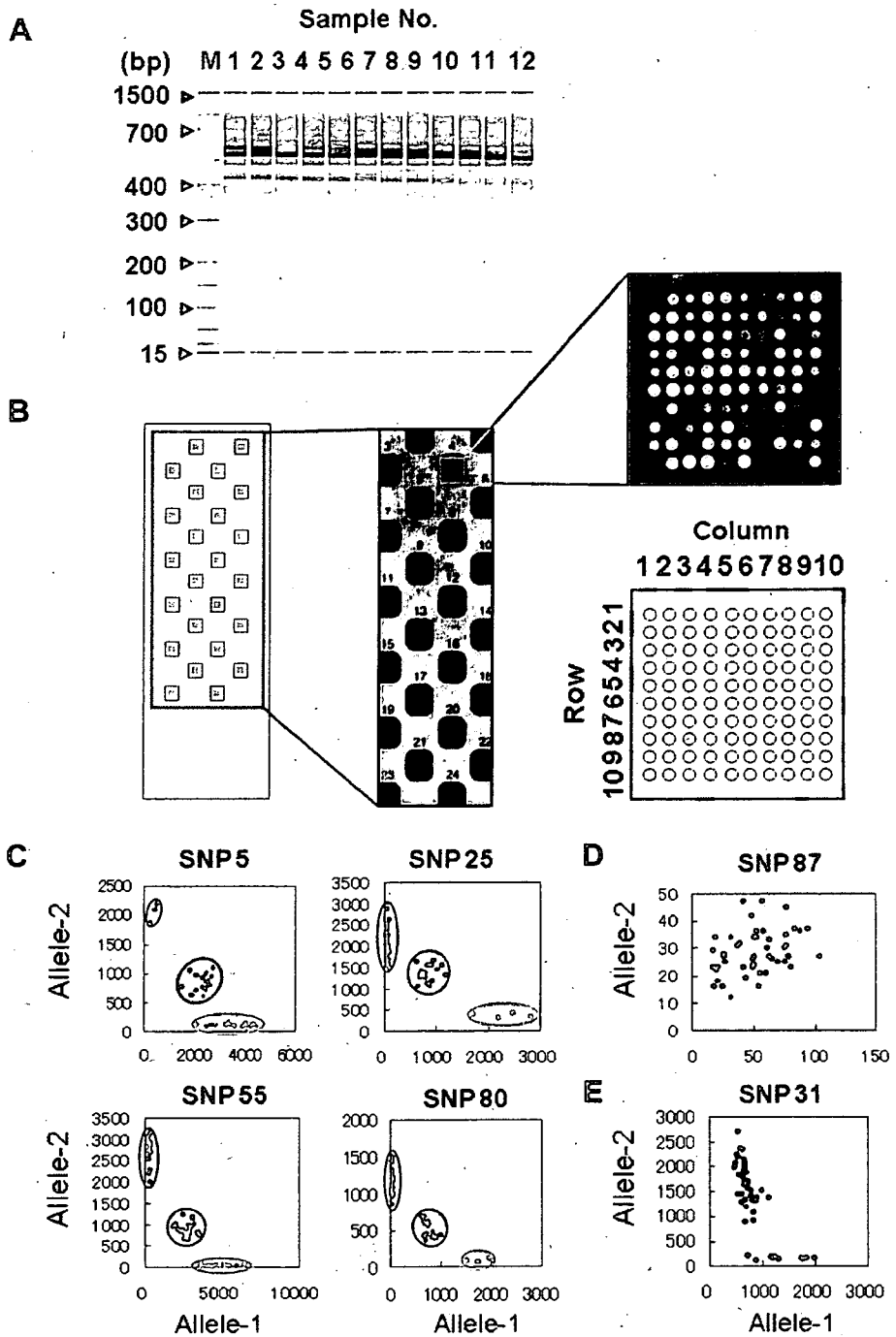

Fig. 4. Multiplex SNP typing for 96 SNPs using 48 individual genomic DNA samples. (A) Gel images of multiplex PCR products with different samples. In all sample lanes, sample bands were observed between two inner markers: 15 and 1500 bp. (B) Hybridization images of DNA microarray. (C) Scatter plot diagrams for 4 randomly selected SNPs from 84 working SNPs. Green dots and circle show allele-1 homozygous samples, red dots and circle show allele-2 homozygous samples, and blue dots and circle show heterozygous samples. (D) Example of the typing-failed SNP caused by insufficient amplification of target fragment in multiplex PCR. (E) Example of the typing-failed SNP that was found to have strong false-positive signals.

reported to be prone to occur when the mismatched pairs are G–T, G–A, G–G, A–G, and T–G [23,24]. Of the 2 misligated SNPs, 1 had an A–G mismatch (SNP 31) and the other had a T–G mismatch (SNP 61) between the 5′ query probe and the target fragment. These 2 SNPs were undetectable, even when 5′ query probes with the mismatched base incorporated into different positions were used (data not shown). Although there were other G–T, G–A, G–G, A–G, and T–G mismatches within the set of 84 working SNPs, we consider that these mismatches would increase the likelihood of misligation in some cases. In the future, we will be able to search for the cause of misligation by

accumulating data from failed analyses of numerous target SNPs.

Conversion rate, call rate, accuracy, and reproducibility

We investigated the feasibility of the DigiTag2 assay by performing 96-plex SNP typing using 48 human genomic DNA samples, and we found that the DigiTag2 assay has the potential to analyze all types of SNP with high accuracy and reproducibility. Here we excluded 7 SNPs from further analysis because they were revealed to be monomorphic in 48 samples. The DigiTag2 assay was found to have a 94.4% (84/89) conversion rate, which is defined as the proportion of successfully genotyped SNPs among the total number of SNPs examined. The call rate, which is defined as the number of genotype calls among the total number of samples examined, was 99.95% (4030/4032) The typing results were 100% identical to the results of direct sequencing. The reproducibility of this assay was examined by duplicate experiments, and it was found that genotype calls were 100% identical between duplicate experiments.

Advantages of DigiTag2 assay

The DigiTag2 assay performs multiplex PCR to excise target regions, including SNP sites from genomic DNA, prior to oligonucleotide ligation assay. Reducing the complexity of the genome by selectively collecting target SNP sites from the genome would lead to successful genotyping [25]. In designing the genotyping probes for oligonucleotide ligation assay, there are no alternatives because the SNP sequence is included in the probe sequences. Therefore, multiplex PCR prior to oligonucleotide ligation assay has an important role in analyzing SNPs that have highly homogeneous regions in the genome. Based on 96-plex SNP typing using 48 individual genomic DNA samples, the DigiTag2 assay has the potential to analyze all types of SNP with high accuracy and reproducibility. Moreover, the DigiTag2 assay uses unmodified primers and probes for target SNPs, thereby reducing assay cost, and requires only simple assay protocols without specialized equipment. We estimated that the running cost for the DigiTag2 assay (for oligonucleotides, reagents, DNA microarrays, etc.) is less than $0.06/genotype. The DigiTag2 assay can use the same set of D1s and EDs for any set of target SNPs, thereby enabling 96-plex genotyping with the same assay protocols and the same microarray having the same set of probes. However, hybridization products, which are prepared in the labeling step, may cross-hybridize to the wrong D1 probes on DNA microarray due to SNP-specific sequences being introduced into the hybridization products. With regard to the 96 target SNPs selected in this study, there is no evidence of cross-hybridization between D1 probes and SNP-specific sequences. Cross-hybridization may be avoided by predicting the interaction between D1 probes and SNP-specific sequences. In the future, we will attempt to predict cross-hybridization by accumulating data from failed analyses of numerous target SNPs.

Acknowledgments

This study was supported by a Grant-in-Aid for Scientific Research on Priority Areas and the New Energy and Industrial Technology Development Organization.

Appendix A. Supplementary data

Supplementary data associated with this article can be found, in the online version, at doi:10.1016/j.ab.2007.02.005.

References

[1] L. Kruglyak, D.A. Nickerson, Variation is the spice of life, Nat. Genet. 27 (2001) 234–236.
[2] M.W. McBride, D. Graham, C. Delles, A.F. Dominiczak, Functional genomics in hypertension, Curr. Opin. Nephrol. Hypertens. 15 (2006) 145–151.
[3] M. Ochi, H. Osawa, H. Onuma, A. Murakami, T. Nishimiya, F. Shimada, K. Kato, I. Shimizu, K. Shishino, M. Murase, Y. Fujii, J. Ohashi, H. Makino, The absence of evidence for major effects of the frequent SNP +299 G > A in the resistin gene on susceptibility to insulin resistance syndrome associated with Japanese type 2 diabetes, Diabetes Res. Clin. Pract. 61 (2003) 191–198.
[4] B.I. Freedman, D.W. Bowden, M.M. Sale, C.D. Langefeld, S.S. Rich, Genetic susceptibility contributes to renal and cardiovascular complications of type 2 diabetes mellitus, Hypertension 48 (2006) 8–13.
[5] R. Yamada, S. Tokuhiro, X. Chang, K. Yamamoto, SLC22A4 and RUNX1: identification of RA susceptible genes, J. Mol. Med. 82 (2004) 558–564.
[6] K. Yamamoto, R. Yamada, Genome-wide single nucleotide polymorphism analyses of rheumatoid arthritis, J. Autoimmun. 25 (2005) 12–15.
[7] N. Tsuchiya, J. Ohashi, K. Tokunaga, Variations in immune response genes and their associations with multifactorial immune disorders, Immunol. Rev. 190 (2002) 169–181.
[8] J. Ohashi, K. Tokunaga, The power of genome-wide association studies of complex disease genes: Statistical limitations of indirect approaches using SNP markers, J. Hum. Genet. 46 (2001) 478–482.
[9] A. Wille, J. Hoh, J. Ott, Sum statistics for the joint detection of multiple disease loci in case-control association studies with SNP markers, Genet. Epidemiol. 25 (2003) 350–359.
[10] C.S. Carlson, M.A. Eberle, L. Kruglyak, D.A. Nickerson, Mapping complex disease loci in whole-genome association studies, Nature 429 (2004) 446–452.
[11] N. Hu, C. Wang, Y. Hu, H.H. Yang, C. Giffen, Z-Z. Tang, X-Y. Han, A.M. Goldstein, M.R. Emmert-Buck, K.H. Buetow, P.R. Taylor, M.P. Lee, Genome-wide association study in esophageal cancer using GeneChip Mapping 10 K Array, Cancer Res. 65 (2005) 2542–2546.
[12] D.J. Schaid, J.C. Guenther, G.B. Christensen, S. Hebbring, C. Rosenow, C.A. Hilker, S.K. McDonnell, J.M. Cunningham, S.L. Slager, M.L. Blute, S.N. Thibodeau, Comparison of microsatellites versus single-nucleotide polymorphisms in a genome linkage screen for prostate cancer-susceptibility loci, Am. J. Hum. Genet. 75 (2004) 948–965.
[13] T. Arinami, T. Ohtsuki, H. Ishiguro, H. Ujike, Y. Tanaka, Y. Morita, M. Mineta, M. Takeichi, S. Yamada, A. Imamura, K. Ohara, H. Shibuya, K. Ohara, Y. Suzuki, T. Muratake, N. Kaneko, T. Someya, T. Inada, T. Yoshikawa, T. Toyota, K. Yamada, T. Kojima, S. Takahashi, O. Osamu, T. Shinkai, M. Nakamura, H. Fukuzako, T. Hashiguchi, S. Niwa, T. Ueno, H. Tachikawa, T. Hori, T. Asada, S. Nanko, H. Kunugi, R. Hashimoto, N. Ozaki, N. Iwata, M. Harano, H. Arai, T. Ohnuma, I. Kusumi, T. Koyama, H. Yoneda, Y. Fukumaki, H. Shibata, S. Kaneko, H. Higuchi, N. Yasui-Furukori, Y. Numachi, M. Itokawa, Y. Okazaki, Japanese Schizophrenia Sib-Pair Linkage

Group, Genome-wide high-density SNP linkage analysis of 236 Japanese families supports the existence of schizophrenia susceptibility loci on chromosomes 1p, 14q, and 20p, Am. J. Hum. Genet. 77 (2005) 937–944.

[14] P.M. Holland, R.D. Abramson, R. Watson, D.H. Gelfand, Detection of specific polymerase chain reaction product by utilizing the 5′→3′ exonuclease activity of *Thermus aquaticus* DNA polymerase, Proc. Natl. Acad. Sci. USA 88 (1991) 7276–7280.

[15] N. Pourmand, E. Elahi, R.W. Davis, M. Ronaghi, Multiplex pyrosequencing, Nucleic Acids Res. 30 (2002) e31.

[16] K. Lindroos, U. Liljedahl, M. Raitio, A-C. Syvänen, Minisequencing on oligonucleotide microarrays: Comparison of immobilisation chemistries, Nucleic Acids Res. 29 (2001) e69.

[17] J. Tost, I.G. Gut, Genotyping single nucleotide polymorphisms by mass spectrometry, Mass Spectrom. Rev. 21 (2002) 388–418.

[18] M.S. Bray, E. Boerwinkle, P.A. Doris, High-throughput multiplex SNP genotyping with MALDI-TOF mass spectrometry: Practice, problems, and promise, Hum. Mutat. 17 (2001) 296–304.

[19] A.R. Tobler, S. Short, M.R. Andersen, T.M. Paner, J.C. Briggs, S.M. Lambert, P.P. Wu, Y. Wang, A.Y. Spoonde, R.T. Koehler, N. Peyret, C. Chen, A.J. Broomer, D.A. Ridzon, H. Zhou, B.S. Hoo, K.C. Hayashibara, L.N. Leong, C.N. Ma, B.B. Rosenblum, J.P. Day, J.S. Ziegle, F.M. De La Vega, M.D. Rhodes, K.M. Hennessy, H.M. Wenz, The SNPlex genotyping system: A flexible and scalable platform for SNP genotyping, J. Biomol. Tech. 16 (2005) 396–404.

[20] N. Nishida, T. Tanabe, K. Hashido, K. Hirayasu, M. Takasu, A. Suyama, K. Tokunaga, DigiTag assay for multiplex single nucleotide polymorphism typing with high success rate, Anal Biochem. 346 (2005) 281–288.

[21] H. Yoshida, A. Suyama, Solution to 3-SAT by breadth first search, DIMACS Ser. Discrete Math. Theor. Comput. Sci. 54 (2000) 9–22.

[22] F. Barany, Genetic disease detection and DNA amplification using cloned thermostable ligase, Proc. Natl. Acad Sci. USA 88 (1991) 189–193.

[23] J.N. Housby, E.M. Southern, Fidelity of DNA ligation: A novel experimental approach based on the polymerisation of libraries of oligonucleotides, Nucleic Acids Res. 26 (1998) 4259–4266.

[24] J. Luo, D.E. Bergstrom, F. Barany, Improving the fidelity of *Thermus thermophilus* DNA ligase, Nucleic Acids Res. 24 (1996) 3071–3078.

[25] H. Matsuzaki, H. Loi, S. Dong, Y-Y. Tsai, J. Fang, J. Law, X. Di, W-M. Liu, G. Yang, G. Liu, J. Huang, G.C. Kennedy, T.B. Ryder, G.A. Marcus, P.S. Walsh, M.D. Shriver, J.M. Puck, K.W. Jones, R. Mei, Parallel genotyping of over 10,000 SNPs using a one-primer assay on a high-density oligonucleotide array, Genome Res. 14 (2004) 414–425.

Severe Toxicities After Irinotecan-Based Chemotherapy in a Patient With Lung Cancer: A Homozygote for the *SLCO1B1*15* Allele

Hiroshi Takane, PhD, Masanori Miyata, MD, PhD,† Naoto Burioka, MD, PhD,† Jun Kurai, MD,† Yasushi Fukuoka, MD, PhD,† Hisashi Suyama, MD, PhD,† Yasushi Shigeoka, MD, PhD,† Kenji Otsubo, PhD,* Ichiro Ieiri, PhD,‡ and Eiji Shimizu, MD, PhD†*

Abstract: Irinotecan is used widely in the treatment of several malignancies, but unpredictable severe toxicities such as myelosuppression and delayed-type diarrhea are sometimes experienced. Polymorphism of the *UGT1A1* gene is one of the likely reasons for interindividual differences in irinotecan pharmacokinetics and severe toxicity. Also, polymorphic organic anion-transporting polypeptide 1B1 (OATP1B1, *SLCO1B1*) is reported to be involved in the hepatocellular uptake of SN-38. A 61-year-old man with lung cancer developed severe toxicities, including grade 3 diarrhea, grade 4 leukopenia, and grade 4 neutropenia, after the first cycle of irinotecan (60 mg/m^2) plus cisplatin chemotherapy. The irinotecan and SN-38 areas under the concentration–time curve from time zero to infinity in this patient were 43% and 87% higher than the corresponding mean values for 10 other patients with lung cancer treated with irinotecan (60–100 mg/m^2) normalized for the dose of irinotecan. Analysis of genetic variants in genes encoding the drug-metabolizing enzyme (*UGT1A1*) and transporter (*SLCO1B1*) involving irinotecan disposition revealed that this patient was homozygous for the *SLCO1B1*15* allele, which may result in severe toxicities attributable to the extensive accumulation of SN-38. Screening of *SLCO1B1*15* is suggested to be useful in irinotecan chemotherapy to avoid unpredicted severe toxicity, although the homozygous genotype is rare among the Japanese.

Key Words: pharmacogenetics, *SLCO1B1*, irinotecan, pharmacokinetics, toxicity

(*Ther Drug Monit* 2007;29:666–668)

INTRODUCTION

Irinotecan (7-ethyl-10-[4-(1-piperidino)-1-piperidino]-carbonyloxycamptothecin [CPT-11]) has displayed promising results in several malignancies such as lung and colorectal cancers. Irinotecan is a camptothecin analog that is mainly converted by carboxylesterase to an active metabolite, SN-38 (7-ethyl-10-hydroxycamptothecin), a potent topoisomerase I inhibitor.[1] Subsequently, SN-38 is conjugated to an inactive glucuronic acid conjugate (SN-38G) by UDP-glucuronosyltransferase 1A1 (UGT1A1).[2] Large interindividual variability in the pharmacokinetics of active metabolite SN-38 is likely important in the clinical outcome and toxicity (including myelosuppression and diarrhea) of irinotecan-based chemotherapy.[3] In particular, interindividual differences in the glucuronidation activity of UGT1A1 have been involved in development of severe toxicities and are explained in part by genetic variation.[4–6] Of the known genetic variants in the *UGT1A1* gene, *UGT1A1*28*, characterized by an extra seventh dinucleotide (TA) insertion in the $(TA)_6$TAA-box in the promoter region, is the most common, leading to decreased converting activity of SN-38 to SN-38G and resulting in increased plasma SN-38 level and severe irinotecan toxicity.[4–6] In addition, *UGT1A1*6* (211G>A)[5] and **60* (−3279T>G)[6] variants have been correlated with a reduction in SN-38 glucuronide formation.

Recently, an in vitro study indicated that SN-38 is a very good substrate for organic anion-transporting polypeptide 1B1 (OATP1B1, *SLCO1B1*), which is expressed on the basolateral membrane in the hepatocytes responsible for the hepatocellular uptake of several compounds from systemic circulation.[7] Previously, we found that the *SLCO1B1*15* (388A>G and 521T>C) variant was associated with a higher plasma concentration of pravastatin, a substrate of OATP1B1.[8] Therefore, to evaluate the contribution of genetic variants in the *UGT1A1* and *SLCO1B1* genes to the variability in irinotecan pharmacokinetics, we performed pharmacokinetic studies at the first administration (cycle) of irinotecan in 11 patients with lung cancer. This study was approved by the Ethics Review Board of Tottori University, and informed consent was obtained from all individuals. We report the case, a patient homozygous for the *SLCO1B1*15* allele, who showed an extensive accumulation of SN-38 after irinotecan administration resulting in severe toxicities.

Received for publication January 22, 2007; accepted April 25, 2007.

From the *Department of Pharmacy, Tottori University Hospital, Yonago; †Division of Medical Oncology and Molecular Respirology, Faculty of Medicine, Tottori University, Yonago; and ‡Department of Clinical Pharmacokinetics, Graduate School of Pharmaceutical Sciences, Kyushu University, Fukuoka, Japan.

This study was supported by Health and Labor Sciences Research Grants from the Ministry of Health, Labor and Welfare, Tokyo, Japan.

H. Takane and M. Miyata contributed equally to this work.

Correspondence: Ichiro Ieiri, PhD, Department of Clinical Pharmacokinetics, Graduate School of Pharmaceutical Sciences, Kyushu University, 3-1-1, Maidashi, Higashi-ku, Fukuoka 812-8582, Japan (e-mail: ieiri-ttr@umin.ac.jp).

TABLE 1. Patient Characteristics

	No.	Sex	Age (Years)	PS	Diagnosis	Dose, mg/m² (On Days) Irinotecan	Cisplatin	*SLCO1B1* *15	*UGT1A1* *60	*28	*6
This case	1	M	61	0	SCLC, ED	60 (1, 8, 15)	60 (1)	+/+	−/−	−/−	−/−
Other patients	2	F	72	0	SCLC, ED	60 (1, 8, 15)	60 (1)	−/−	−/−	−/−	−/−
(nos. 2–11)	3	M	78	0	SCLC, ED	60 (1)	–	−/−	−/−	−/−	−/−
	4	F	53	0	NSCLC, Sq	80 (1)	–	−/+	−/−	−/−	−/−
	5	M	80	2	NSCLC, Sq	100 (1)	–	−/+	−/−	−/−	−/−
	6	M	64	0	SCLC, ED	60 (1, 8, 15)	60 (1)	−/−	−/+	−/+	−/−
	7	M	50	0	SCLC, LD	60 (1, 8, 15)	60 (1)	−/+	−/+	−/+	−/−
	8	M	40	0	NSCLC, Ad	60 (1, 8, 15)	80 (1)	−/−	+/+	−/+	−/−
	9	M	67	0	NSCLC, Ad	80 (1)	–	−/−	+/+	−/−	−/−
	10	M	53	0	NSCLC, Ad	60 (1, 8, 15)	60 (1)	−/+	−/−	−/−	−/+
	11	M	58	2	SCLC, ED	100 (1)	–	−/+	−/−	−/−	−/+

M, male; F, female; PS, performance status; SCLC, small-cell lung cancer; NSCLC, nonsmall-cell lung cancer; ED, extensive disease; LD, limited disease; Ad, adenocarcinoma; Sq, squamous cell carcinoma.

SCLC is commonly staged using the VA Lung Cancer Group staging system.[9] This system classifies patients into LD or ED. LD is defined as disease confined to one hemithorax, in the absence of a malignant effusion, with disease that can be encompassed in one radiation port. Disease that does not meet this criteria is defined as ED.

CASE REPORT

A 61-year-old man (Eastern Cooperative Oncology Group performance status 0) was admitted to our hospital and diagnosed with small-cell lung cancer (extensive disease[9]) (Table 1). He was treated with irinotecan (60 mg/m² on days 1, 8, and 15) in combination with cisplatin (60 mg/m² on day 1) of a 28-day cycle as second-line treatment. Irinotecan was administered in the presence of oral alkalization (sodium bicarbonate, magnesium oxide, metoclopramide, and ursodeoxycholic acid) to reduce irinotecan-induced delayed diarrhea. He had also received lansoprazole, rebamipide, allopurinol, and mosapride. Toxicity was graded according to the Common Terminology Criteria for Adverse Events, version 3.0. After the first cycle of chemotherapy, he developed severe side effects, including grade 3 diarrhea (day 15), grade 4 leukopenia (day 14), and grade 4 neutropenia (day 14), and then required the continuous administration of granulocyte-colony stimulating factor and antibiotics; therefore, chemotherapeutic treatment on day 15 was discontinued. In the control group (ie, patient nos. 2–11, Table 1), patient no. 7 (grade 4 neutropenia and grade 3 diarrhea), and patient no. 8 (grade 4 neutropenia) were experiencing serious adverse effects during the first cycle of chemotherapy, but all were manageable.

Blood samples (each of 2 mL) for all enrolled patients with lung cancer were obtained at 0.5, 1, 1.5, 2, 4, 8, 12, and 24 hours after the start of irinotecan infusion (90-minute intravenous infusion) on day 1 of the first cycle. Serum concentrations of total irinotecan, SN-38, and its glucuronide (SN-38G) at the first administration of irinotecan were measured by high-performance liquid chromatography according to previously described methods.[10,11]

The areas under the concentration–time curve from time zero to infinity (AUCs) of irinotecan, SN-38, and SN-38G in this patient were 4553.2, 260.7, and 864.4 ng × hr/mL, respectively. The pharmacokinetic parameters of irinotecan were compared with 10 other patients with lung cancer receiving irinotecan (Table 2). The irinotecan and SN-38 AUCs (ng × hr/mL) normalized by the dose (mg/m²) of irinotecan in this patient (75.9 and 4.3) were 43% and 87%

TABLE 2. Pharmacokinetics of Irinotecan and Its Metabolites in the Case and 10 Other Patients

	*SLCO1B1*15*			
	*15/*15	−/− or −/*15		
Pharmacokinetic Parameters	**Case**	**Patient Nos. 2–5**	**Patient Nos. 6–11**	**Patient Nos. 2–11**
CLcr (mL/min)	71.8	64.5 ± 18.0	87.3 ± 12.8	78.2 ± 18.1
Total bilirubin (mg/mL)	0.5	0.4 ± 0.1	0.4 ± 0.2	0.4 ± 0.2
AST (IU/L)	28.0	24.0 ± 11.5	26.8 ± 11.3	25.7 ± 10.8
ALT (IU/L)	31.0	18.5 ± 8.3	24.7 ± 11.8	22.2 ± 10.5
$CL_{irinotecan}$ (L/hr/m²)	13.2	16.4 ± 1.1	19.7 ± 2.8	18.4 ± 2.8
$AUC_{irinotecan}$/dose	75.9	58.5 ± 5.0	49.5 ± 6.2	53.1 ± 7.2
AUC_{SN-38}/dose	4.3	1.6 ± 0.4	2.8 ± 0.6*	2.3 ± 0.8
AUC_{SN-38G}/dose	14.4	9.8 ± 3.7	7.4 ± 2.2	8.4 ± 2.9
REC ($AUC_{SN-38}/AUC_{irinotecan}$)	0.057	0.028 ± 0.009	0.057 ± 0.014*	0.045 ± 0.019
REG (AUC_{SN-38G}/AUC_{SN-38})	3.3	6.2 ± 1.3	2.4 ± 0.7*	3.9 ± 2.1

Genetic characteristics of the *UGT1A1* gene are summarized in Table 1.

Each value is expressed as the mean ± standard deviation.

CLcr, creatinine clearance; CL, total clearance; AUC/dose, area under the concentration–time curve from time zero to infinity (ng × hr/mL) normalized by dose (mg/m²); REC, relative extent of conversion of irinotecan into SN-38; REG, relative extent of glucuronidation to SN-38 into SN-38G.

*$P < 0.05$ when compared with the group including patient nos. 2–5 was analyzed with Mann-Whitney U test.

higher than the corresponding mean values for the other 10 patients (53.1 and 2.3) (Table 2). Plasma concentrations of irinotecan and SN-38 in this case were remarkably higher than those in other patients.

Genotyping of *UGT1A1*6* was performed by polymerase chain reaction–restriction fragment length polymorphism methods as previously reported.[4] Also, *UGT1A1*28* and **60* were determined with polymerase chain reaction–single-strand conformation polymorphisms or direct sequencing using gene-specific primers (5′-AAGTGAACTCCCTGCTACCTT-3′ [forward primer] and 5′-CC ACTGGGATCAACAGTATCT-3′ [reverse] for *UGT1A1*28* and 5′-GTCATAGTAAGCTGGCCAAGGGTAGAG-3′ [forward] and 5′-CA TCGGCTGCCCACCTGAATAAA-3′ [reverse] for *UGT1A1*60*). This patient did not harbor any of these variants in the promoter and the coding regions of the *UGT1A1* gene (Table 1). Haplotyping of *SLCO1B1*15* was identified according to previously described methods.[8] In the *SLCO1B1* gene, this patient was a homozygous carrier of the *SLCO1B1*15* allele (Table 1).

SN-38 is metabolized to SN-38 glucuronide by hepatic UGT1A1 and excreted into feces (8.24% of dose) and urine (3.02%).[12] Severe hematologic and gastric toxicities are sometimes observed in patients homozygous for the *UGT1A1**28 allele,[4,6] but this genotyping pattern was not found in our patients. The AUC ratio of SN-38G to SN-38 (relative extent of glucuronidation to SN-38 into SN-38G, 3.3) in this case was lower than that in four other patients (patient nos. 2–5, group 1) with a reference allele for the *UGT1A1* gene (6.2 ± 1.3, mean ± standard deviation) as homozygosity and comparable with six other patients (patient nos. 6–11, group 2) harboring at least one variant allele of the *UGT1A1* gene (2.4 ± 0.7) (Table 2). These results suggest that glucuronidation capability was not the major determinant of the severe toxicities observed in this patient.

Irinotecan is mainly converted by carboxylesterase 2 (CE-2) to an active metabolite, SN-38. Functional genetic polymorphisms in the *CE-2* gene are extremely rare (0.3%) in the Japanese.[13] The AUC ratio of SN-38 to irinotecan in this patient (relative extent of conversion of irinotecan into SN-38, 0.057) was higher (0.028) than and comparable (0.057) with the mean values in patients in group 1 and group 2, respectively (Table 2). In addition to CE-2, irinotecan is known to be metabolized by CYP3A4 to form inactive metabolites.[14] Coadministration of the CYP3A4 inhibitor may lead to the increasing formation of SN-38[15]; however, none of our patients was receiving medications known to interact with irinotecan. Furthermore, no patients with both renal and liver dysfunctions were included in this study (Table 2). These findings suggest that the higher plasma concentrations of irinotecan and SN-38 in this case could not be explained by the functional deficiency of either metabolizing enzyme.

Nozawa et al[7] reported that OATP1B1 transports SN-38, but not irinotecan and SN-38G in HEK293 cells, and demonstrated that the *SLCO1B1*15* allele exhibits decreased transport activities for SN-38 in *Xenopus* oocytes. In contrast to these in vitro findings, this patient, who was homozygous for the *SLCO1B1*15* allele, showed higher plasma concentrations of SN-38 and irinotecan than the mean values of 10 other patients, including five heterozygous carriers of the *SLCO1B1*15* allele. These results were consistent with the findings of Xiang et al.[16] However, in the present study, we did not observe significant differences in irinotecan (noncarriers, 51.4 ± 7.4; heterozygosity, 54.7 ± 7.3), SN-38 (noncarriers, 2.3 ± 0.7; heterozygosity, 2.3 ± 1.0), and SN-38G (noncarriers, 8.4 ± 4.2; heterozygosity, 8.4 ± 1.4) AUCs normalized by the dose of irinotecan between noncarriers and heterozygous carriers of the *SLCO1B1*15* allele, possibly attributable to the small sample size of the study and mismatched genotypes of the *UGT1A1* polymorphisms. Although the reasons for the discrepancy between previous in vitro and our in vivo findings are not clear, this case suggests that the low transport activity of OATP1B1 leads to increased not only SN-38, but also irinotecan exposure in humans.

This is the first report suggesting that homozygosity of the *SLCO1B1*15* allele is important for the variability in irinotecan and SN-38 dispositions and is implicated in the unpredicted accumulation of plasma SN-38, resulting in irinotecan-related severe toxicities. In the present study, contribution of comedicated cisplatin to the observed toxicities could not be excluded; however, low transport activity of OATP1B1 attributable to the *SLCO1B1*15* allele may lead to increased systemic exposure of SN-38 by reduced hepatocellular uptake of SN-38 from the systemic circulation. Although the frequency of homozygous carriers of *SLCO1B1*15* is low (0.8% in the Japanese),[8] genotyping of this variant may be useful to avoid severe toxicities after irinotecan treatment with a standard body surface area-based dose.

REFERENCES

1. Kawato Y, Aonuma M, Hirota Y, et al. Intracellular roles of SN-38, a metabolite of camptothecin derivative CPT-11, in the antitumor effect of CPT-11. *Cancer Res.* 1991;51:4187–4191.
2. Iyer L, King CD, Whitington PF, et al. Genetic predisposition to the metabolism of irinotecan (CPT-11): Role of uridine diphosphate glucuronosyltransferase isoform 1A1 in the glucuronidation of its active metabolite (SN-38) in human liver microsomes. *J Clin Invest.* 1998;101: 847–854.
3. Mathijssen RHJ, van Alphen RJ, Verweij J, et al. Clinical pharmacokinetics and metabolism of irinotecan (CPT-11). *Clin Cancer Res.* 2001;7: 2182–2194.
4. Ando Y, Saka H, Ando M, et al. Polymorphisms of UDP-glucuronosyltransferase gene and irinotecan toxicity: a pharmacogenetic analysis. *Cancer Res.* 2000;60:6921–6926.
5. Sai K, Saeki M, Saito Y, et al. UGT1A1 haplotypes associated with reduced glucuronidation and increased serum bilirubin in irinotecan-administered Japanese patients with cancer. *Clin Pharmacol Ther.* 2004; 75:501–515.
6. Kitagawa C, Ando M, Ando Y, et al. Genetic polymorphism in the phenobarbital-responsive enhancer module of the UDP-glucuronosyltransferase 1A1 gene and irinotecan toxicity. *Pharmacogenet Genomics.* 2005;15:35–41.
7. Nozawa T, Minami H, Sugiura S, et al. Role of organic anion transporter OATP1B1 (OATP-C) in hepatic uptake of irinotecan and its active metabolite, 7-ethyl-10-hydroxycamptothecin: in vitro evidence and effect of single nucleotide polymorphisms. *Drug Metab Dispos.* 2005; 33:434–439.
8. Nishizato Y Nishizato, Ieiri I, Suzuki H, et al. Polymorphisms of *OATP-C* (*SLC21A6*) and *OAT3* (*SLC22A8*) genes: consequences for pravastatin pharmacokinetics. *Clin Pharmacol Ther.* 2003;73:554–565.
9. Zelen M. Keynote address on biostatistics and data retrieval. *Cancer Chemother Rep 3.* 1973;4:31–42.
10. Rivory LP, Robert J. Identification and kinetics of a β-glucuronide metabolite of SN-38 in human plasma after administration of the camptothecin derivative irinotecan. *Cancer Chemother Pharmacol.* 1995; 36:176–179.
11. Sparreboom A, de Bruijn P, de Jonge JA, et al. Liquid chromatographic determined of irinotecan and three major metabolites in human plasma, urine and feces. *J Chromatogr B.* 1998;721:225–235.
12. Slatter JG, Schaaf LJ, Sams JP, et al. Pharmacokinetics, metabolism, and excretion of irinotecan (CPT-11) following i.v. infusion of [^{14}C] CPT-11 in cancer patients. *Drug Metab Dispos.* 2000;28:423–433.
13. Kim S, Nakamura T, Saito Y, et al. Twelve novel single nucleotide polymorphisms in the CES2 gene encoding human carboxylesterase 2 (hCE-2). *Drug Metab Pharmacokinet.* 2003;18:327–332.
14. Santos A, Zanetta S, Createil T, et al. Metabolism of irinotecan (CPT-11) by CYP3A4 and CYP3A5 in humans. *Clin Cancer Res.* 2000;5:2012–2020.
15. Kehrer DFS, Mathijssen RHJ, Verweij J, et al. Modulation of irinotecan metabolism by ketoconazole. *J Clin Oncol.* 2002;20:3122–3129.
16. Xiang X, Jada SR, Li HH, et al. Pharmacogenetics of SLCO1B1 gene and the impact of *1b and *15 haplotypes on irinotecan disposition in Asian cancer patients. *Pharmacogenet Genomics.* 2006;16:683–691.